Journal of Organometallic Chemistry, 350 (1988) 191–205
Elsevier Sequoia S.A., Lausanne – Printed in The Netherlands

Isolation, characterisation, and solution structures of the bis(pyridine) complex of the n-butyllithium-pyridine adduct, $Bu^n(C_5H_5N)Li \cdot 2C_5H_5N$, its mode of decomposition, and ab initio calculations on model systems

David R. Armstrong, Robert E. Mulvey,

Department of Pure and Applied Chemistry, University of Strathclyde, Glasgow G1 1XL (Great Britain)

Donald Barr, Ronald Snaith *

University Chemical Laboratory, Lensfield Road, Cambridge CB2 1EW (Great Britain)

and David Reed

Department of Chemistry, University of Edinburgh, Edinburgh EH9 3JJ (Great Britain)

(Received February 26th, 1988)

Abstract

The complexed adduct, $Bu^n(C_5H_5N)Li \cdot 2C_5H_5N$ (**3**) has been isolated from the reaction of Bu^nLi with a 3-fold molar excess of pyridine, and characterised fully by analysis and by ^1H, ^{13}C NMR spectroscopy. Ab initio calculations on model systems have shown that the formation of **3** probably involves initial complexation of the organolithium to the pyridine nitrogen atom, and that subsequent addition to the aromatic ring is aided by the presence of donor (pyridine) molecules. Cryoscopic molecular mass measurements imply that adduct **3** is essentially monomeric in arene solution, so that the 1/1/1 ^7Li NMR resonances observed at low temperatures can be provisionally attributed to conformers arising due to the presence of chiral ($Bu^nC_5H_5N$)-nitrogen and -C(2) centres. High-field ^1H NMR spectra of solutions of **3** of various ages and of various thermal/photochemical histories have shown that conversion of **3** into 2-butylpyridine (**1**) proceeds at least in part via hydrolysis to 1,2-dihydro-2-butylpyridine (**4**).

Introduction

Since 1930 it has been known that reactions of organolithiums such as n-butyllithium with pyridine lead ultimately to 2-substituted products, e.g., 2-n-butylpyridine (**1**) [1], and it has generally been assumed that such reactions proceed via adducts like **2**, usually represented as the delocalised ionic form [2]. More recently, such adducts were said to be "isolated and characterised" [3], though in fact the

0022-328X/88/$03.50

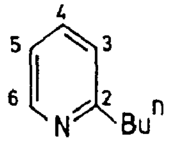

(1)

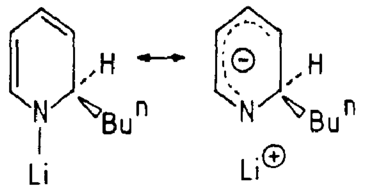

(2)

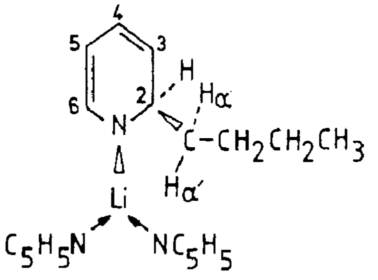

(3)

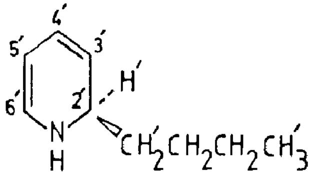

(4)

study involved synthesis of insoluble yellow products from reactions of Bu^{n}Li or PhLi with pyridine or substituted pyridines in ether, followed by their take-up in TMEDA and ^{1}H NMR investigations of resulting solutions: indeed, it was noted that good elemental analyses of the adducts themselves were precluded by their extreme air- and heat-sensitivities. A related study involved direct preparation of a 1 : 1 reaction solution of Bu^{n}Li and pyridine in ether, this solution being stable for several hours at room temperature or for several weeks at $-78\,^\circ$C; once more, the addition product was not isolated, but instead was investigated by low-temperature ^{1}H NMR solution spectroscopy [4]. Several other relevant papers have concerned reactions of organolithium-pyridine adducts with electrophiles such as acid chloride and alkyl halides, and the thermal and catalytic decompositions of these adducts [5].

In this paper, aspects of which have appeared in preliminary form [6,7], we report the actual isolation and characterisation of a crystalline bis(pyridine) complex of the Bu^{n}Li : pyridine adduct **3**, prepared readily by reaction of Bu^{n}Li with an excess of pyridine. Product **3** has been shown to be essentially monomeric in arene solutions, and analyses of its ^{1}H, ^{13}C, and ^{7}Li NMR spectra permit conclusions about its structure and about the electronic effects of organolithium addition to the precursor pyridine ring; these latter conclusions have been backed up by results from ab initio MO calculations on model systems. Furthermore, the ^{1}H NMR spectra of solutions of **3** recorded under diverse conditions shed light on the mechanism of conversion of **2** or **3** into **1**, pointing in particular to the intermediacy of the dihydrobutylpyridine (**4**).

Results and Discussion

Addition of Bu^nLi in hexane to a chilled three-fold molar excess of pyridine in hexane produced a clear orange solution on warming to room temperature. After refrigeration overnight, a batch of large yellow crystals formed and were identified as the bis(pyridine) complex of the 1 : 1 Bu^nLi : pyridine adduct, viz. 2-$Bu^nC_5H_5NLi \cdot (C_5H_5N)_2$ (**3**). In this high yield preparation, therefore, pyridine acts not only as a reactant in the usual sense, but also as a Lewis base which helps to stabilise, and certainly to crystallise and to solubilise, the addition product; cf. the above-noted NMR studies [2,3] where the species being examined in solution were presumably TMEDA and bis(Et_2O) complexes of the addition products. The clear preference for attachment of two donor pyridine molecules to each Li in the adduct is emphasised by the observation that a 1 : 2 $Bu^nLi : C_5H_5N$ reaction system produces a mixture of **3** and the yellow, insoluble uncomplexed adduct, **2**. In this context, organoN-Li complexes with monodentate donors have hitherto had 1 : 1 stoichiometry, such species then dimerising and so attaining 3-coordination for their Li centres, e.g., $[Bu^t_2C{=}NLi \cdot O{=}P(NMe_2)_3]_2$, [8] and $[(Me_3Si)_2NLi \cdot OEt_2]_2$ [9]. However, molecular models for a 1 : 1 complex 2-$Bu^nC_5H_5NLi \cdot C_5H_5N$ show, not surprisingly, that dimerisation would be impossible sterically; presumably therein lies the preference for attachment of two pyridine Lewis base molecules per Li, this being an alternative way for each Li to acquire 3-coordination.

Complex-adduct **3** is extremely air- and moisture-sensitive, and seemingly heat- and light-sensitive also: the yellow crystals can be kept for many weeks in foil-wrapped flasks in a refrigerator, but exposure to light and/or storage at ambient temperatures rapidly causes darkening, first to orange then to deep red/brown. Such sensitivities may reflect the coordinatively unsatisfied nature of the Li centres within **3**, linked to the monomeric state of the species. For such reasons, maybe reinforced by the fact that addition across N(1)=C(2) of pyridine has produced an asymmetric C(2) centre so allowing the possibility of conformers (see below), it has so far proved impossible to obtain a single crystal amenable to X-ray diffraction study. Nonetheless, much can be deduced about the structural nature of **3**. Firstly, its likely monomeric state in the solid is manifest in arene solutions, cryoscopic measurements in benzene giving association state values (n) of 0.86 (for a 4.5×10^{-2} mol dm^{-3} solution, expressed relative to the empirical formula, i.e., $n = 1$), 0.74 (3.8×10^{-2} mol dm^{-3}), and 0.71 (1.5×10^{-2} mol dm^{-3}). Such results suggest that the expected solid-state monomer with an intact (though highly polar) N–Li bond largely persists on dissolution, though with some dissociation of donor pyridine, particularly so in more dilute solutions. They do not support fully ionic formulations involving contact and separated ion-pairs, $Bu^nC_5H_5N^- \cdot Li^+(C_5H_5N)_2$ and $Bu^nC_5H_5N^- \cdots Li^+(C_5H_5N)_2$ respectively, for which n values near 0.5 in very dilute solutions would be expected. Furthermore, such ionic equilibria would lead to particularly concentration-dependent ^7Li NMR δ values, but such are not observed [7]. The ^1H NMR spectrum (250.13 MHz) of a relatively dilute solution (31 mg cm^{-3}, 1.0×10^{-1} mol dm^{-3}) of freshly-isolated **3** in toluene-d_8 at 25 °C is shown in Fig. 1, and details are recorded in Table 1 alongside those for 2-$Bu^n(C_5H_5N)Li$ in Et_2O at −78 °C [4]. Such a spectrum proves conclusively the purity and identity of **3**, there being three typical signals representing the ten protons of the two pyridine donor molecules (4H/2H/4H, little shifted from their positions in the spectrum of

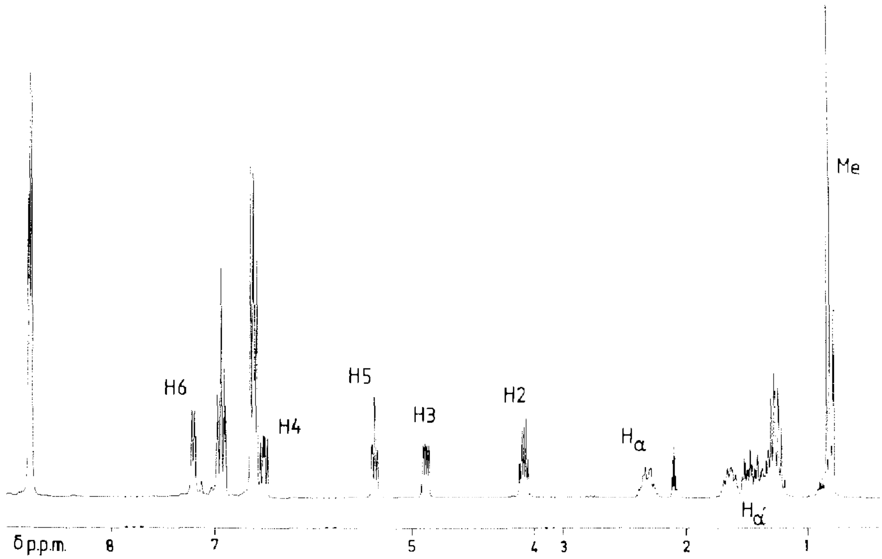

Fig. 1. ^{1}H NMR (250.13 MHz) spectrum of freshly-isolated **3** in toluene-d_8 at 25 °C, 31 mg cm^{-3}, 1.0×10^{-1} mol dm^{-3}.

free pyridine), five clearly separate signals due to the five protons of the reduced pyridine ring (H(2)–H(6)), and a series of resonances assigned to the nine n-butyl protons. One of these latter resonances (H_α) is quite distinct, the diastereotopic α-methylene protons, ($CH_\alpha H_{\alpha'}$), being anisochronous. All assignments and cou-

Table 1

^{1}H NMR assignments and parameters for n-butyllithium-pyridine adducts

Assignment [c]	2-Bu^n(C$_5$H$_5$N)Li [a]			2-Bu^n(C$_5$H$_5$)NLi·(C$_5$H$_5$N)$_2$ (**3**) [b]		
	Multiplicity δ (ppm)	Relative integral	J_{xy} (Hz)	Multiplicity δ (ppm)	Relative integral	J_{xy} (Hz)
H(6)	d, 6.68	1H	J_{56} 5.8	d, 7.17	1H	J_{56} 5.6
H(4)	d of d, 5.93	1H	J_{34} 8.2 J_{45} 5.4	d of d, 6.58	1H	J_{34} 8.4 J_{45} 5.6
H(5)	t of d, 4.62	1H	J_{56} 5.8 J_{45} 5.4 (J_{35} 0.8)	t of d, 5.29	1H	J_{56} 5.6 J_{45} 5.6 (J_{35} 1.3)
H(3)	d of d, 4.34	1H	J_{34} 8.2 J_{23} 4.2	d of d, 4.87	1H	J_{34} 8.4 J_{23} 4.3
H(2)	d, 3.64	1H	J_{23} 4.2	d of d of d, 4.07	1H	$J_{2\alpha}$ 8.9 $J_{2\alpha'}$ 4.3 J_{23} 4.1
H_α	–	–	–	poorly resolved m, 2.30	1H	$J_{2\alpha}$ 8.9 $J_{\alpha\alpha'}$ – $J_\alpha CH_2$ –
$-CH_{\alpha'}CH_2CH_2CH_3$	–	–	–	m, 1.70–1.18	5H	–
$-CH_{\alpha'}CH_2CH_2CH_3$	–	–	–	t, 0.81	3H	–

[a] In Et$_2$O, −70 °C. Reference [4]. [b] In toluene-d_8, 25 °C. Pyridine donor resonances at δ 8.66 (m, 4H; H(2), H(6)), δ 6.94 (m, 2H; H(4)), δ 6.67 (m, 4H; H(3), H(5)); [c] See **2** for numbering scheme.

Table 2

^{13}C NMR assignments and parameters for pyridine, 4-methylpyridine, and their butyllithium adducts

Assignment	4-MeC$_5$H$_4$N [a] δ (ppm)	2-Bu^n(MeC$_5$H$_4$N)Li [a] δ (ppm) [c]	C$_5$H$_5$N [b] δ (ppm)	2-Bu^n(C$_5$H$_5$N)Li ·(C$_5$H$_5$N)$_2$ (3) [b] δ (ppm) [c]
C(6)	149.6	148.7(−0.9)	150.6	150.0(−0.6)
C(4)	146.4	132.6(−13.8)	136.0	127.8(−8.2)
C(3)	124.3	96.6(−27.7)	124.1	100.8(−23.3)
C(5)	124.3	93.2(−31.1)	124.1	93.9(−30.2)
C(2)	149.6	56.4(−93.2)	150.6	57.6(−93.0)

[a] In THF, 75.4 MHz, 20 °C. From ref. 5. [b] In benzene-d_6, 25.15 MHz, 25 °C. Pyridine donor resonances at 150.8 (C(2), C(6)); 136.6(C(4)); 124.1(C(3,5)); [c] δ(pyridine adduct) − δ(pyridine) in parentheses.

plings for **3** were verified by individual proton decoupling of each resonance in turn. The only major difference between the two sets of results shown in Table 1 for **3** and for (presumably) its Et$_2$O-complexed analogue lies in the *observed* non-equivalence of the butyl α-C(H$_\alpha$H$_{\alpha'}$) protons within the former species: thus, for **3**, H(2) couples not only with H(3) but also, all to different extents, with H$_\alpha$ and H$_{\alpha'}$.

As was noted earlier [4] (excluding the signal from H(2) whose pyridine C(2) atom has been re-hybridised to sp^3) the major shifts of proton resonances in these adducts compared to their positions in pyridine itself occur for H(3) and H(5) (Table 1). Assuming a fully ionic formulation, Bu^n(C$_5$H$_5$N)$^-$ · Li$^+$, such movements have been interpreted [4] in terms of a total of 0.2e$^-$ of the extra negative charge being localised equally at positions 3 and 5, leaving 0.8e$^-$ on N; MO calculations at various levels have implied similar charge distributions [10]. Not unexpectedly, rather complementary ^{13}C chemical shift movements also occur, as shown in Table 2 for **3** cf. pyridine, and for the 1 : 2 addition product of 4-methylpyridine with Bu^{n}Li cf. 4-methylpyridine [5]. It is apparent that, leaving aside the re-hybridised C(2), the most drastic chemical shift movements occur again at ring positions 3 and 5 (though in fact C(5) moves slightly more to low frequency than does C(3)).

To probe these structural and electronic alterations further, and in particular to estimate the true extent (< 100%) of the ionic character of such adducts, and to gauge the separate charge distributions on C and H ring atoms, we have carried out ab initio MO calculations on a series of model species, **5–10**. The 6-31G basis set was used to examine the electronic structures of **5–8**, products and ammonia-complexed products of reactions of pyridine with LiH (used here as a model for butyllithium), while the smaller basis set STO-3G was invoked to investigate the structures of adducts Me(C$_5$H$_5$N)Li (**9**) and Bu^n(C$_5$H$_5$N)Li (**10**).

Details of the optimised geometries of, and charge distributions within, LiH · C$_5$H$_5$N species **5–8** are given in Table 3. The corresponding values for pyridine itself are included for comparison, and these show that the C$\doteq$C bond lengths are almost equal (1.39 Å) while the C$\doteq$N ones span 1.33 Å. The charge distributions within pyridine indicate that there is a small polarisation of charge away from all the H atoms, that the observed large movement of charge to N is mainly due to σ-electron drift (0.39e$^-$) with just a small π-electron contribution (0.12e$^-$), and that there is a smaller build-up of charge at C(3) and at C(5). Clearly, from these results, any reaction between pyridine and a lithium compound (such as LiH) is expected to

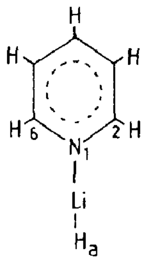

(5)

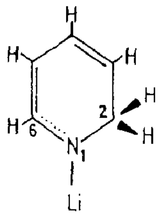

(6)

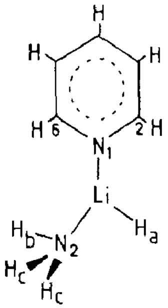

(7)

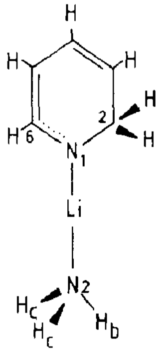

(8)

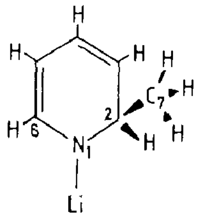

(9)

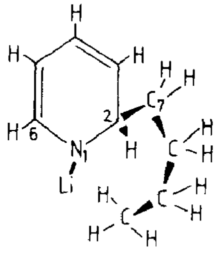

(10)

initially take place at the nitrogen, giving a donor–acceptor species with a coordinate N → Li bond. For such a species, **5**, the resulting stabilisation energy is calculated to be 27.7 kcal mol^{-1} with respect to the separated reactants. The optimised geometrical parameters of **5** show that the geometry of the pyridine moiety is only slightly perturbed and that the moiety retains its aromatic character; the Li–H bond is weakened by coordination to pyridine, and the N–Li bond length of 2.02 Å is in the range expected for a bond formed by a two-coordinate Li atom [11]. There is a small movement of charge ($\sim 0.1e^-$) from pyridine to the LiH portion and within pyridine there has been a greater polarisation of charge due to formation of **5**, most significantly an electron drift from the α(CH) units, 2 and 6, to the N atom. Such results indicate that, in a reaction between an oligomeric

Table 3

The optimised bond lengths and electron distribution of pyridine and its donor–acceptor complexes and adducts with LiH

	C_5H_5N	$LiH \cdot C_5H_5N$ (5)	$H_3N \cdot LiH \cdot C_5H_5N$ (7)	$H(C_5H_5N)Li$ (6)	$H(C_5H_5N)Li \cdot NH_3$ (8)
Principal bond lengths (Å)					
N(1)- C(2)	1.33	1.38	1.34	1.48	1.48
C(2)- C(3)	1.39	1.39	1.39	1.51	1.51
C(3)- C(4)	1.39	1.39	1.39	1.34	1.33
C(4)- C(5)	1.39	1.39	1.39	1.45	1.45
C(5)- C(6)	1.39	1.39	1.38	1.36	1.36
C(6)- N(1)	1.33	1.38	1.34	1.37	1.36
N(1)- Li	–	2.02	2.05	1.79	1.83
Li- H_a	–	1.67	1.74	–	–
C(2)- H(2)	1.08	1.08	1.08	1.10	1.10
Li- N(2)	–	–	2.07	–	2.04
N(2)-H_b	–	–	1.01	–	1.01
N(2)-H_c	–	–	1.01	–	1.01
Bond indices					
N(1)-C(2)	1.56	1.48	1.49	1.05	1.05
C(2)-C(3)	1.48	1.49	1.48	1.05	1.06
C(3)-C(4)	1.49	1.48	1.49	1.89	1.93
C(4)-C(5)	1.49	1.48	1.47	1.14	1.13
C(5)-C(6)	1.48	1.49	1.49	1.70	1.67
C(6)-N(1)	1.56	1.48	1.49	1.34	1.37
Li-H_a	–	0.95	0.91	–	–
C(2)-H(2)	0.92	0.90	0.89	0.92	0.92
N(2)-H_b	–	–	0.94	–	0.93
N(2)-H_c	–	–	0.92	–	0.93
Charges					
N(1)	−0.51	−0.74	−0.71	−1.02	−0.99
C(2)	+0.14	+0.23	+0.22	+0.11	+0.11
H(2)	+0.14	+0.18	+0.23	+0.10	+0.09
C(3)	−0.20	−0.20	−0.20	−0.27	−0.28
H(3)	+0.13	+0.15	+0.14	+0.09	+0.09
C(4)	−0.06	−0.04	−0.04	−0.05	−0.05
H(4)	+0.14	+0.16	+0.15	+0.09	+0.09
C(5)	−0.20	−0.20	−0.21	−0.32	−0.33
H(5)	+0.13	+0.15	+0.14	+0.08	+0.07
C(6)	+0.14	+0.23	+0.21	+0.29	+0.30
H(6)	+0.14	+0.18	+0.16	+0.09	+0.09
Li	–	+0.17	+0.11	+0.70	+0.57
H_a	–	−0.26	−0.34	–	–
N(2)	–	–	−0.76	–	−0.78
H_b	–	–	+0.27	–	+0.31
H_c	–	–	+0.31	–	+0.31

organolithium, $(RLi)_n$, and pyridine, both reagents are activated towards addition across α-C=N by initial formation of a N → Li donor–acceptor species: the former's C–Li bond would be lengthened and made more polar, i.e., more "carbanionic" (plus also n is probably reduced, so increasing the kinetic activity of the organolithium), while the latter's αC-atoms would be rendered less negative, so priming them to add R^- in a subsequent step.

The consequences of such a step, i.e., cleavage of the Li–H bond in **5** (which, to give $C_5H_5N \cdot Li^+$ alone, would require 160 kcal mol^{-1}) with concomitant formation of an α-C–H bond, have been probed by optimisation of structure **6**, $H(C_5H_5N)Li$. Two possible geometries were considered. In the first case, a plane of symmetry was present while for the second case no symmetry constraints were imposed. The latter geometry was calculated to be more stable by a mere 2 kcal mol^{-1}, and the bond length variation between the two possible structures was found to be less than 0.01 Å; the main differences occur at the CH_2 portion, which in the C_1 structure is distorted with respect to the rest of the pyridine ring, and at the N–Li bond, which is displaced from the plane. The essential geometrical feature common to both structures is that the equivalence of the C–C bonds, so the aromaticity of the pyridine ring, has been destroyed, and in **6** we now have two near-single and two near-double C–C bonds as shown by their lengths (1.51, 1.45 Å; 1.34, 1.36 Å) and by their bond indices (1.05, 1.14; 1.89, 1.70). The presence of two hydrogen atoms at α-C(2) has reduced the positive charge of this carbon compared to that in pyridine, although the second α-C(6) atom is more positively charged. Atoms C(3) and, especially, C(5) have gained more electron density, in line with large shifts to lower frequency noted earlier for their NMR resonances (Table 2). The nitrogen atom carries a large negative charge which has emanated mainly from the lithium.

Structure **6**, although 10.2 kcal mol^{-1} more stable than the separated reactants, is 17.5 kcal mol^{-1} less stable than the structure of **5**, the donor–acceptor species. However, it might be expected that solvation of the lithium of structure **6** would reduce this energy difference between **5** and **6**. To probe this expectation, we examined structures **7** and **8**, the ammonia complexes of **5** and **6** respectively; the NH_3 mimics (one of) the donor C_5H_5N molecules in **3**. In **7**, the effect of NH_3 complexation to the donor–acceptor species **5** is to stabilise **5** by a further 14.8 kcal mol^{-1}, i.e., the energy difference between **7** and its separated components (C_5H_5N, LiH, NH_3) is now -42.5 kcal mol^{-1}. The addition of NH_3 to Li lengthens the pyridine N–Li bond by 0.05 Å and the Li–H bond by 0.07 Å: thus, such complexation is priming the Li–H bond for dissociation. Further addition of donor molecules will obviously aid this process and moreover will decrease the angles at Li, in turn decreasing the distance between the αC atom and the leaving group, i.e., H^- in this case. For **8**, the NH_3 complex of the adduct **6**, we imposed a plane of symmetry on the structure in order to reduce the computational effort. The result of complexation is to stabilise **6** by 26.0 kcal mol^{-1}, so that the energy difference between **8** and its three separated components is -36.2 kcal mol^{-1}. Hence the energy preference for **5** over **6**, 17.5 kcal mol^{-1}, becomes, after NH_3 addition, i.e., for **7** over **8**, 6.3 kcal mol^{-1}. One can reasonably expect, then, that addition of a *second* NH_3 donor molecule to Li (cf. the presence of two C_5H_5N molecules in **3**) would result in the complexed adduct, $H(C_5H_5N)Li \cdot 2$(donor), being *more* stable than the complexed donor–acceptor species, $C_5H_5N \cdot LiH \cdot 2$(donor): hence one can rationalise the isolation of **3** rather than that of $C_5H_5N \cdot Bu^nLi \cdot 2(C_5H_5N)$. Interestingly, also, in **8** the NH_3 (whose presence does not radically alter the C_5H_5N structural framework) donates $0.14e^-$ to the complex and most of this is retained by the Li, with the pyridineN–Li bond lengthening to 1.83 Å. Hence complexation reduces the polar character of an adduct such as **2** or **6**, supporting our earlier contention that complexed adducts such as **3** or **8** are best thought of as species with intact, highly polar N–Li bonds rather than as ion-separated species.

To examine the effects of organolithium RLi (rather than LiH) addition to pyridine, the optimised geometries of Me(C_5H_5N)Li (**9**) and of Bu^n(C_5H_5N)Li (**10**) were obtained using the minimum basis set (STO-3G), and the results are presented in Table 4. The geometry of the C_5H_5N ring in both **9** and **10** is very similar, with the expected single and double C–C bonding pattern present. In **10** lithium is positioned slightly closer to C(2) [Li $\cdots$ C = 2.72 Å in **10**] than to C(6) [Li $\cdots$ C = 2.79 Å in **10**] and moreover it is aligned with the C(2)–H bond rather than with the C(2)–R one so that the Li $\cdots$ H distance is of length 2.76 Å with an associated bond index of 0.012. These features in general may be compared with the usual, pictorial ways of depicting organolithium-pyridine adducts (e.g., compare **10** with **2**); the noted Li $\cdots$ H contact in particular may also go some way towards explaining apparently facile LiH elimination from, e.g., **10**, **2**, to give e.g., **1**.

The charge distributions show a similar pattern within **9** and **10**, with the Li donating electron density principally to the pyridine N atom. The charges on the carbon atoms within the pyridine ring exhibit an order of increasing negative charge C(2) < C(6) < C(4) < C(3) < C(5) and, apart from C(2) which has a different coordination number, this order can be correlated with the previously-noted order of the ^{13}C chemical shifts of **3**. The hydrogen atoms of the ring are all positively charged, but there is no easily identifiable relationship between these charge densities and the ^{1}H NMR chemical shifts observed. The hydrogen atoms on the side chain are also positively charged while the alkyl carbons are negatively charged, and these combine to give a small negative charge (ca. 0.01–0.02e^-) on the alkyl side chain.

As a final part of this study we have attempted to ascertain the mode of decomposition of the complexed adduct **3** to the 2-substituted pyridine **1** by recording the high-field ^{1}H NMR spectra of solutions of **3** of various ages and of various thermal and photochemical histories. The spectrum of freshly-isolated crystals of **3** dissolved in toluene-d_8 has already been referred to (Fig. 1). Figures 2 and 3 show ^{1}H NMR spectra (360.13 MHz) of other solutions of **3**, this time made up from crystals a week old which had been stored in the dark, but at room temperature. The spectrum of a relatively dilute solution (31 mg cm^{-3}, 1.0×10^{-1} mol dm^{-3}; Fig. 2) shows firstly that, scanning from high to low frequency, signals due to H(6), H(5), H(3) and Me (cf. Fig. 1) now have nearby, but much smaller (ca. 1/8) signals (primed) of the same multiplicity; the same is probably true for H(4), with its sister signal (H(4′)) being partly obscured by a (donor) pyridine resonance. Visual similarities apart, these like-signals have been confirmed as H(6′), H(5′), H(3′), and Me′ by individual decoupling experiments, e.g., H(6′) is indeed coupled to H(5′) only, as was H(6) to H(5). Furthermore, the signals for H(2) and H_α also have smaller signals in their vicinity, but these are, in contrast, of markedly different shapes and multiplicities, viz. near H(2) there is a doublet (H(2′), δ 4.06 ppm, ca. 1/8th of the integral of H(2)) and a single resonance (δ 3.90 ppm, ~ 1/8th also), and near H_α there is a triplet (δ 2.66 ppm, ~ 1/4th of the integral of H_α). Specific proton decoupling has shown that the doublet H(2′) is coupled only to H(3′) (cf. H(2) was coupled to H(3), *and* to H_α and $H_{\alpha'}$ of the n-butyl α-CH_2 unit), while the triplet is coupled to one of the CH_2 resonances in the region δ 1.6–1.2 ppm (cf. H_α was coupled to a CH_2, *and* to H(2) and to $H_{\alpha'}$). On the basis of these experiments, all these additional (primed) signals can be assigned to 1,2-dihydro-2-butylpyridine

Table 4

The optimised bond lengths and electron distribution of Me(C_5H_5N)Li and Bu(C_5H_5N)Li

	Me(C_5H_5N)Li **(9)**	Bu(C_5H_5N)Li **(10)**
Principal bond lengths (Å)		
N(1)–C(2)	1.50	1.50
C(2)–C(3)	1.53	1.53
C(3)–C(4)	1.31	1.32
C(4)–C(5)	1.47	1.47
C(5)–C(6)	1.33	1.33
C(6)–N	1.42	1.41
N–Li	1.69	1.69
C(2)–C(7)	1.57	1.57
C(7)–C(8)	–	1.55
C(8)–C(9)	–	1.55
C(9)–C(10)	–	1.54
Bond indices		
N(1)–C(2)	0.99	0.99
C(2)–C(3)	1.00	1.00
C(3)–C(4)	1.90	1.89
C(4)–C(5)	1.08	1.08
C(5)–C(6)	1.76	1.76
C(6)–N	1.14	1.15
C(2)–C(7)	0.99	0.97
C(7)–C(8)	–	1.00
C(8)–C(9)	–	1.00
C(9)–C(10)	–	1.00
Charges		
N(1)	−0.32	−0.33
Li	+0.33	+0.27
C(2)	+0.06	+0.05
H(2)	+0.04	+0.04
C(3)	−0.08	−0.09
H(3)	+0.05	+0.04
C(4)	−0.07	−0.06
H(4)	+0.05	+0.05
C(5)	−0.14	−0.14
H(5)	+0.04	+0.04
C(6)	+0.05	+0.05
H(6)	+0.04	+0.03
C(7)	−0.17	−0.10
H(7)	+0.05, +0.05, +0.06	+0.05, +0.04
C(8)	–	−0.10
H(8)	–	+0.06, +0.06
C(9)	–	−0.09
H(9)	–	+0.06, +0.06
C(10)	–	−0.18
H(10)	–	+0.08, +0.07, +0.05

(4) as follows: H(6′)–H(3′) to the ring protons as shown, the single resonance to N*H*, the doublet to H(2′) (now only observed to couple to H(3′), and not to the α-CH_2' group), and the triplet to the α-CH_2' protons (still inequivalent, but now

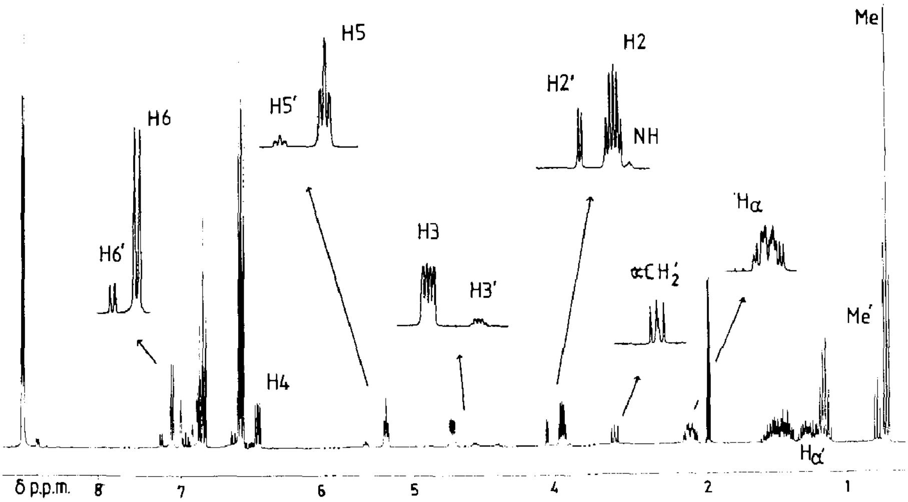

Fig. 2. ^{1}H NMR (360.13 MHz) spectrum of a one-week old sample of 3 in toluene-d_8 at 25 °C, 31 mg cm^{-3}, 1.0×10^{-1} mol dm^{-3}.

only observed to couple to the β-CH_2 unit). The triplet near Me is clearly due to Me′, and the outermost multiplets in the range δ 1.6–1.2 ppm are due to the β,γ-CH_2CH_2 units: the central multiplet here has, like H_α, diminished in intensity (cf. Fig. 1) on appearance of α-CH_2', and so can be assigned to $H_{\alpha'}$ in **3**. One noteworthy implication of these results is that the chemical shift non-equivalence of the diastereotopic butyl group α-methylene protons, $CH_\alpha H_{\alpha'}$, was enhanced in **3** by the presence of the $Li \cdot (C_5H_5N)_2$ unit, so giving observed couplings of H_α and $H_{\alpha'}$ to each other and, separately, to H(2).

Although the integrals can only be approximate, it seems that the hydrolysis product **4** is present to the extent of ca. 12% in this relatively dilute solution of **3**. The origin of this trace hydrolysis can be attributed to storage, even in a glove-box operating at ca. 2 ppm H_2O, and/or to atmospheric moisture admitted during the sealing of NMR tubes, and/or to residual moisture in even spectroscopic-grade,

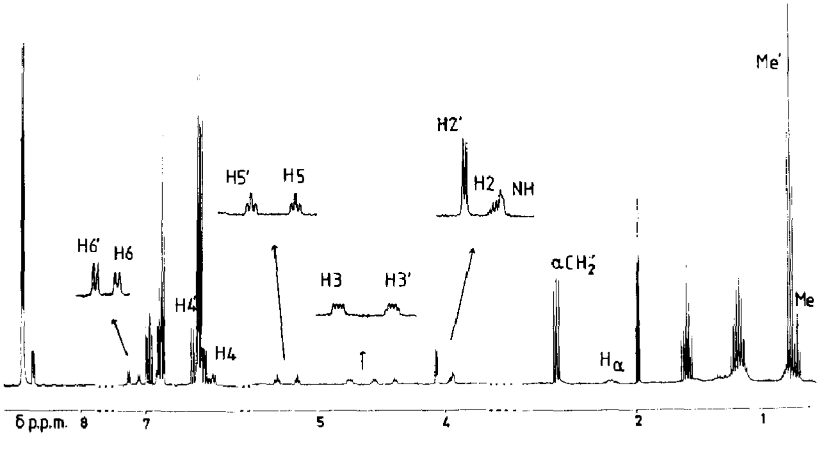

Fig. 3. ^{1}H NMR (360.13 MHz) spectrum of a one-week old sample of 3 in toluene-d_8 at 25 °C, 67 mg cm^{-3}, 2.2×10^{-1} mol dm^{-3}.

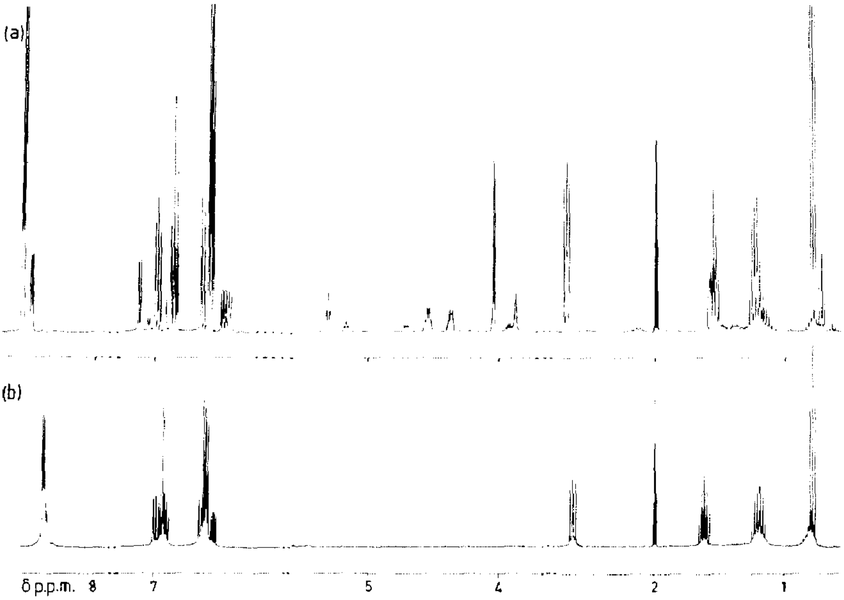

Fig. 4. (a) ^1H NMR spectrum of the solution referred to in Fig. 3 after exposure to light for several hours. (b) ^1H NMR spectrum of the solution in (a) after brief exposure to the atmosphere.

molecular-sieved deuterated NMR solvents. Such factors make total exclusion of moisture unavoidable, though they do permit monitoring of the processes that occur during the synthetically-useful conversion of **2**, **3** to **1**. Perhaps surprisingly, hydrolysis of **3** seems to occur more extensively in concentrated solutions, and it certainly does so on exposure of the solutions to light, when they darken rapidly. Figure 3 depicts the ^1H NMR spectrum of a more concentrated (67 mg cm^{-3}; 2.2×10^{-1} mol dm^{-3}) solution of **3**, again, as for Fig. 2, prepared from a week-old sample of **3** which had been stored in the dark. It is apparent that considerable hydrolysis of **3** to **4** has taken place, with (primed) resonances due to the latter being, if anything, larger than (unprimed) ones due to the former; it is also noteworthy that the growth of the triplet due to α-CH_2' has been accompanied by a diminution not only of H_α but also of the central of the three butyl multiplets (cf. with Figs. 1, 2), so confirming its assignment to $H_{\alpha'}$ in **3**. After exposure of this same concentrated solution (still in a sealed tube, under nitrogen) to daylight for several hours, when it darkens to near-black, the re-recorded spectrum (Fig. 4(a)) shows that the changes just noted have been much exacerbated in that **4** is now the major solution component. After opening this NMR tube to the atmosphere for several minutes, then re-accumulating the spectrum, it is found (Fig. 4(b)) that all the signals due to **3**, *and* those due to **4**, have disappeared: this final spectrum is that of 2-butylpyridine (**1**). At the same time, the air-exposed solution becomes cloudy, presumably due to formation and precipitation of LiOH: certainly a Nujol mull of complex **3** exposed to the atmosphere for several seconds affords an IR spectrum which is a superimposition of the spectra of free pyridine (bands shifted relative to those in **3**), of **1** (with minor traces of residual **4**), and of LiOH [ν Li(O–H) sharp, at 3680 cm^{-1}]. The implications of these results are that conversion of **2**, or its complexed versions such as **3**, into **1** does not, or does not exclusively, occur in a single step via LiH elimination, but that slight hydrolysis, possibly photochemically-encouraged,

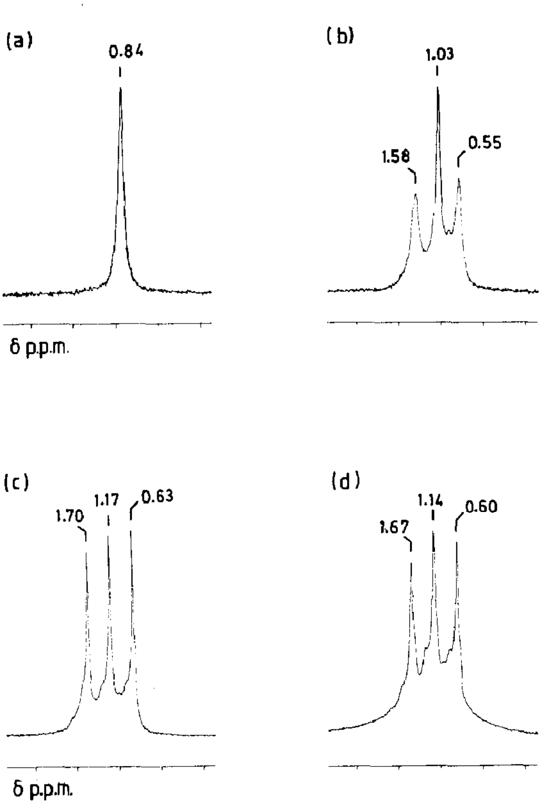

Fig. 5. ^{7}Li NMR (139.96 MHz) spectra of solutions of **3** (a) 15 mg cm^{-3}, 5.0×10^{-2} mol dm^{-3}, at −30 °C; (b) at −60 °C; (c) at −95 °C; (d) 120 mg cm^{-3}, 4.0×10^{-1} mol dm^{-3}, at −95 °C.

produces **4** which then rapidly eliminates dihydrogen, or otherwise disproportionates, to give **1**.

For completeness, some preliminary attempts have been made to scrutinise the solution behaviour of **3** using variable-temperature ^{7}Li NMR (139.96 MHz) spectroscopy. We have already reported [7], as part of a ^{7}Li NMR study of organonitrogen-lithium compounds in general, that a benzene-d_6 solution of **3** at 20 °C gives rise to a single, sharp ^{7}Li resonance (δ 0.33 ppm). Initially, a singlet persists on cooling, e.g., at −30 °C for a dilute (15 mg cm^{-3}, 5.0×10^{-2} mol dm^{-3}) solution in toluene-d_8, a singlet at δ 0.84 ppm is observed (Fig. 5(a)). However, at −60 °C, the spectrum is much more complex and three dominant signals are apparent (Fig. 5(b)); the same signals are also present (at δ 1.54, 1.01, and 0.52 ppm), and in roughly the same proportions, in the −60 °C spectrum of a much more concentrated (120 mg cm^{-3}, 4.0×10^{-1} mol dm^{-3}) solution. Both −60 °C spectra are temperature-reversible, with coalescence of the signals being observed at ca. −45 °C. By −95 °C, these three signals have sharpened, and the outer ones have intensified to give roughly 1/1/1 relative integrals (Fig. 5(c), dilute solution); once more, though, these observations apply equally well to the −95 °C spectrum of the much more concentrated solution (Fig. 5(d)). The origin of these three low-temperature signals for **3** remains uncertain at present, and has not so far been clarified by low-temperature ^{1}H and ^{13}C NMR experiments (in which rather broad and indistinct resonances have been observed). However, it seems very unlikely that the three 1/1/1 ^{7}Li NMR signals at −95 °C arise on account of the presence of three different association states of **3**: firstly as these signals are markedly concentration independent, and secondly, as discussed earlier, in view of the results of cryoscopic measurements and of the steric improbability of, e.g., dimer formation. Similarly, for several reasons, it seems improbable that the three signals are due to **3** itself and to **3** minus variable amounts of its two C_5H_5N donor molecules: firstly, because the *two* outer signals at −60 °C (Fig. 5(b)) intensify on *lowering* the temperature (a process which should discourage dissociation of donor pyridines), secondly because at −95 °C a roughly 1/1/1 signal integration is maintained for solutions differing in concentration by a factor of 8 (Fig. 5(c), (d)), and thirdly because a cryoscopic association state value (n) of 0.86 was observed, albeit at ca. 6 °C, for the NMR "dilute" solution (Fig. 5(c)), so that, for the 8-fold more-concentrated NMR solution, a n value close to 1, i.e., with *no* dissociation of pyridine, could confidently be expected. The possible explanations remaining hinge around the facts that both the (pyridine)C(2) and pyridineN(1) centres are chiral ones, so that we may be observing here low-temperature diastereoisomeric conformers of monomeric **3**; further low temperature NMR studies with isotopic enrichment (^{13}C, ^{15}N) are planned to explore this likelihood.

Experimental

Synthesis of $Bu^n(C_5H_5N)Li \cdot 2C_5H_5N$ (3)

n-Butyllithium (2.1 cm^3 of a 1.57 mol dm^{-3} solution in hexane, 3.3 mmol) was added to a chilled solution of pyridine (0.79 g, 10 mmol) in hexane (10 cm^3). The mixture was allowed to warm to room temperature to give a clear orange solution. This was kept for several hours at −10 °C, giving yellow crystals which were filtered off, washed with chilled hexane, and identified as the above compound. Yield, 0.87 g, 88%; m.p. 70–72 °C. Anal. Found: C, 75.6; H, 8.2; Li, 2.5; N, 13.1. $C_{19}H_{24}LiN_3$ calc: C, 75.8; H, 8.0; Li, 2.3; N, 14.0%.

IR spectrum: 1622w, 1594s, 1573ms, 1484vs, 1442vs, 1365ms, 1342m, 1318m, 1285m, 1218ms, 1152ms, 1117m, 1105m, 1094m, 1070ms, 1034s, 1003ms, 993m, 982m, 966m, 950m, 926m, 905m, 885w, 876w, 841w, 754ms, 750ms, 708vs, 701vs, 666w, 654w, 636ms, 619s, 579vs (cm^{-1}; Nujol mull).

After brief air-exposure bands assignable to ν(Li)O–H, at 3680 cm^{-1}, and to ν(N–H) of **4**, at 3315 cm^{-1}, appeared in the spectrum. Spectra were recorded on a Perkin–Elmer 457 grating spectrometer.

NMR spectra: ^{7}Li (139.96 MHz) spectra were measured on a Bruker WH 360 NMR spectrometer, ^{7}Li chemical shifts (δ) being quoted relative to external phenyllithium in toluene-d_8 (Θ value, 38.863 882 MHz). Proton spectra were recorded on Bruker WH 360 (360.13 MHz) and WH 250 (250.13 MHz) instruments, proton shifts being given relative to $SiMe_4$. ^{13}C spectra were obtained on a JEOL PS-100-PFT spectrometer, using $SiMe_4$ as an internal standard. All solutions were prepared in a glove-box and tubes subsequently sealed under nitrogen.

Cryoscopic molecular mass measurements on benzene solutions of **3** were carried out as described previously [7]. For MO calculations, the optimised geometries described were obtained from the ab initio computer program GAMESS [12] using the 6-31G basis set [13] and the STO-3G basis set [14].

Acknowledgements

We thank the SERC (D.B., R.S.) and the Royal Society (R.E.M.) for financial support, and the SERC for the use of high-field NMR facilities.

References

1 K. Ziegler and H. Zeiser, Chem. Ber., 63 (1930) 1847.
2 R.A. Abramovitch and G.A. Poulton, Chem. Comm., (1967) 274.
3 C.S. Giam and J.L. Stout, Chem. Comm., (1969) 142.
4 G. Fraenkel and J.W. Cooper, Tetrahedron Lett., (1968) 1825.
5 C.S. Giam, E.E. Knaus and F.M. Pasutto, J. Org. Chem., 39 (1974) 3565; R.F. Francis, C.D. Crews and B.S. Scott, ibid., 43 (1978) 3227; R.F. Francis, W. Davis and J.T. Wisener, ibid., 39 (1974) 59.
6 D. Barr, R. Snaith, R.E. Mulvey and D. Reed, Polyhedron, 7 (1988) 665.
7 D. Reed, D. Barr, R.E. Mulvey and R. Snaith, J. Chem. Soc., Dalton Trans., (1986) 557.
8 D. Barr, W. Clegg, R.E. Mulvey, D. Reed and R. Snaith, Angew. Chem. Int. Ed. Engl., 24 (1985) 328.
9 M.F. Lappert, M.J. Slade, A. Singh, J.L. Atwood, R.D. Rogers and R. Shakir, J. Am. Chem. Soc., 105 (1983) 302; L.M. Engelhardt, A.S. May, C.L. Raston and A.H. White, J. Chem. Soc., Dalton Trans., (1983) 1671.
10 R. Hoffmann, J. Chem. Phys., 39 (1963) 1397; J.A. Pople and G.A. Segal, ibid., 44 (1966) 3289.
11 W. Setzer and P.v.R. Schleyer, Adv. Organomet. Chem., 24 (1985) 353.
12 M. Dupuis, D. Spangler and J.J. Wendoloski, "GAMESS", N.R.C.C. Software Catalogue, Vol. 1, Program No 2 GO1, 1980; M.F. Guest, J. Kendrick and S.A. Pope, GAMESS Documentation, Daresbury Laboratory, 1983.
13 W.J. Hehre, R. Ditchfield and J.A. Pople, J. Chem. Phys., 56 (1972) 2257; P.C. Hariharan and J.A. Pople, Theor. Chim. Acta, 28 (1973) 213; J.D. Dill and J.A. Pople, J. Chem. Phys., 62 (1975) 2921.
14 W.J. Hehre, R.F. Stewart and J.A. Pople, J. Chem. Phys., 51 (1969) 2657; W.J. Hehre, R. Ditchfield, R.F. Stewart and J.A. Pople, ibid., 52 (1970) 2769.